Hourglass Control for Linear and Nonlinear Problems

T.B. Belytschko, W.K. Liu
Department of Civil Engineering, The Technological Institute, Northwestern University, Evanston, Illinois 60201, U.S.A.

J.M. Kennedy
Reactor Analysis and Safety Division, Argonne National Laboratory, 9700 South Cass Avenue, Argonne, Illinois 60439, U.S.A.

ABSTRACT

Many explicit time integration codes employ quadrilateral elements in two dimensions and hexahedral elements in three dimensions with one-point quadrature [1-3]. Finite difference methods based on the contour integral technique [4] employ similar equations [5]. One-point quadrature provides tremendous benefits in nonlinear algorithms because the number of evaluations of the semidiscretized gradient operator, commonly known as the $\underset{\sim}{B}$ matrix, and the constitutive equations, is reduced substantially. For example, in two dimensions, full-quadrature generally requires 4 integration points, while in three dimensions, it requires 8 quadrature points. Recent studies suggest that the rate of convergence of the one-point quadrature element is comparable to that of the fully integrated elements. Furthermore, the fully integrated elements tend to lock if the behavior of the material becomes incompressible. For these reasons, there appears to be little benefit in using full integration.

The major drawback of one-point quadrature in these elements is a mesh instability often known as hourglassing, which were first recognized in the finite difference literature [6]. They are a special case of the phenomenon known in finite elements as kinematic modes or spurious zero-energy modes; see for example Irons and Ahmad [7]. Numerous techniques have been developed for the control of the hourglass mode in the four node quadrilateral and the corresponding two dimensional finite difference equations used in Lagrangian finite differences codes. One of the earliest of these is the technique developed by Maenchen and Sack [6] who added artificial viscosity to inhibit opposing rotations of the sides of the quadrilateral zone. A finite element version of the Maenchen and Sack antihourglass viscosity has been developed by Belytschko and Kennedy [7]. Alternative methods have been developed in [4] and [8-11]. In this paper, an hourglass procedure which is not activated by rigid body modes is described. Some solutions of the diffusion equation (both linear and nonlinear) are presented.

1. INTRODUCTION

The development of an effective hourglass control requires that the resistance be more general than a simple viscosity; also, the hourglass generalized strains and stresses should not be activated in rigid body motion [10]. This requirement can be considered an orthogonality condition, for it implies that the hourglass operator is orthogonal to rigid body motion. A simple and unique form of this operator for both the 4-node quadrilateral and the 8-node hexahedron for 30 problems has been given in [11], where the hourglass operator was developed by subtracting the effect of the bilinear portion of the velocity field. In this paper, the hourglass projection is obtained more elegantly by simply using the consistency requirements derived in [11] and enforcing certain conditions suggested by the rank deficiency of the discrete forms of the gradient operators. Secondly its application to nonlinear problems is studied.

For the sake of brevity, only the Laplace (diffusion) equation will be treated. It has the same characteristics as the two and three dimensional equations of solid mechanics, yet enables the salient features and characteristics of hourglass modes and their control to be clearly demonstrated. Some results obtained by this procedure are given in Section 4 for both linear and nonlinear problems.

2. HOURGLASS CONTROL FOR LAPLACE EQUATION

Throughout this paper, standard indicial notation will be used, so repeated subscripts imply summation over the range of that subscript. Subscripts which follow a comma denote spatial derivatives.

Consider the Laplace equation

$$\alpha u_{,ii} + s = 0 \tag{1}$$

where u is the dependent variable, α the diffusivity, and s the dimensionless source term. As is well known, see for example [14], the finite element discretization of (1) can be written as

$$\underset{\sim}{K}\ \underset{\sim}{u} + \underset{\sim}{f} = 0 \tag{2}$$

where $\underset{\sim}{K}$ is assembled from the element stiffnesses $\underset{\sim}{K}^e$ which are given by

$$K^e_{IJ} = \int_{V_e} \alpha N_{I,i} N_{J,i} \, dV \tag{3}$$

where V_e is the volume of the element and N_I are the shape functions which give the independent variable in the element by

$$u(\underset{\sim}{x}) = N_I (\underset{\sim}{x})\ \underset{\sim}{u}^e_I \tag{4}$$

where $\underset{\sim}{x}$ are the spatial coordinates.

If we use the standard, isoparametric shape functions in conjunction with one-point quadrature of the right hand side of Eq. (3) to evaluate $\underset{\sim}{K}^e$ for a 4 node quadrilateral,

we obtain

$$\underset{\sim}{K}^e = \alpha A \underset{\sim}{b}_i \underset{\sim}{b}_i^T \qquad \underset{\sim}{b}_i = \underset{\sim}{N}_{,i} \tag{5}$$

where A is the area of the element and

$$\underset{\sim}{b}_1 = \frac{1}{2A} [y_{24}, y_{31}, y_{42}, y_{13}] \tag{6a}$$

$$\underset{\sim}{b}_2 = \frac{1}{2A} [x_{42}, x_{13}, x_{24}, x_{31}] \tag{6b}$$

$$A = \frac{1}{2} (x_{31}y_{42} + x_{24}y_{31}) \tag{6c}$$

with x_I, y_I the coordinates of the node I.

Note that the matrix $\underset{\sim}{B}$, given by

$$\underset{\sim}{B} = \begin{Bmatrix} \underset{\sim}{b}_1^T \\ \underset{\sim}{b}_2^T \end{Bmatrix} \tag{7a}$$

is the discrete counterpart of the gradient operator. The gradient and flux matrices in the finite element approximation are given by

$$\underset{\sim}{g} = \begin{Bmatrix} u_{,x} \\ u_{,y} \end{Bmatrix} = \underset{\sim}{B}\, \underset{\sim}{u}^e \qquad \underset{\sim}{q} = \begin{Bmatrix} q_x \\ q_y \end{Bmatrix} \qquad \underset{\sim}{q} = -\alpha\, \underset{\sim}{g} \tag{7b}$$

The following additional column vectors are useful

$$\underset{\sim}{s}^T = [1, 1, 1, 1] \qquad \underset{\sim}{h}^T = [1, -1, 1, -1] \tag{8a}$$

$$\underset{\sim}{x}_1 = \underset{\sim}{x} = [x_1, x_2, x_3, x_4] \qquad \underset{\sim}{x}_2 = \underset{\sim}{y} = [y_1, y_2, y_3, y_4] \tag{8c}$$

It can be easily verified from Eqs. (6) and (8) that

$$\underset{\sim}{b}_i^T \underset{\sim}{x}_j = \delta_{ij} \tag{9}$$

where δ_{ij} is the Kronecker delta.

Remark. Equation (9) is an important necessary requirement for the rows of the gradient matrix $\underset{\sim}{B}$. It is the counterpart of the consistency conditions in finite difference equations and the gradient of a linear field is evaluated properly only if it is satisfied.

Additional conditions which follow from Eqs. (6) and (8) are

$$\underset{\sim}{b}_i^T \underset{\sim}{s} = 0 \qquad \underset{\sim}{s}^T \underset{\sim}{h} = 0 \tag{10}$$

For any nondegenerate quadrilateral, $\underset{\sim}{b}_i$, $\underset{\sim}{s}$ and $\underset{\sim}{h}$ are linearly independent and span the 4 dimensional space R^4.

The orthogonality properties, Eqs. (10), allow us to quickly examine the pathology of this element that results from one-point quadrature. If we let the nodal values of $\underset{\sim}{u}^e$ for an element be given by $\underset{\sim}{s}$, then

$$\underset{\sim}{g} = \underset{\sim}{B}\ \underset{\sim}{u}^e = \underset{\sim}{B}\ \underset{\sim}{s} = 0 \tag{11}$$

where the last step in the above follows from Eqs. (5) and (10a). This result is expected and in fact necessary since it indicates that for a constant field u, the gradient vanishes. The one-dimensional space spanned by the vector $\underset{\sim}{s}$ will be called the proper null-space of $\underset{\sim}{B}$.

If we let $\underset{\sim}{u}^e = \underset{\sim}{h}$, Eqs. (5) and (10b) again show that $\underset{\sim}{g} = 0$. This result is quite unexpected since the field associated with these nodal values is obviously not constant. The contradictory nature of this result can be appreciated further by noting that for a square element, with all nodes at +1 and -1, $\underset{\sim}{u}^e = \underset{\sim}{h}$ corresponds to $u(x,y) = xy$, yet Eqs. (7) and (10b) show that discrete gradient of this field vanishes. The one-dimensional space spanned by $\underset{\sim}{h}$ will be called the improper null-space of $\underset{\sim}{B}$.

This suggests that the pathology of this element may be eliminated by defining an additional gradient $\hat{g}$ by

$$\hat{g} = \chi^T\ \underset{\sim}{u}^e \tag{12}$$

The discrete gradient operator of Eq. (7a) performs properly on linear fields, which can be seen by letting $\underset{\sim}{u}^e = \underset{\sim}{x}$ or $\underset{\sim}{u}^e = \underset{\sim}{y}$ and using Eqs. (9). Thus χ should not distort the behavior of $\underset{\sim}{B}^*$ or $\underset{\sim}{K}^e$ on linear fields. Therefore χ will be chosen so that :

i. for any nodal values associated with linear fields, $\hat{g} = 0$

ii. if $\underset{\sim}{u}^e$ is in the improper null-space, $\hat{g} \neq 0$.

To obtain χ, we expand it in terms of the base vectors of R^4 as follows

$$\chi = a_1\ \underset{\sim}{b}_1 + a_2\ \underset{\sim}{b}_2 + a_3\ \underset{\sim}{s} + a_4\ \underset{\sim}{h} \tag{13}$$

For an arbitrary linear field, the nodal values are given by

$$\underset{\sim}{u}^e = c_1\ \underset{\sim}{x} + c_2\ \underset{\sim}{y} + c_3\ \underset{\sim}{s} \tag{14}$$

Substituting Eqs. (13) and (14) into Eq. (12) and using Eqs. (9) and (10) yields

$$\chi = \frac{1}{A}\ [\ h - (\underset{\sim}{h}^T\ \underset{\sim}{x})\ \underset{\sim}{b}_1 - (\underset{\sim}{h}^T\ \underset{\sim}{y})\ \underset{\sim}{b}_2] \tag{15}$$

This χ differs in magnitude from that given in [11] but is otherwise identical.

The generalized gradient $\hat{g}$ is associated with a generalized flux $\hat{q}$; the two are related by

$$\hat{q} = -\hat{\alpha}\,\hat{g} = -\varepsilon\,\alpha\,\hat{g} \qquad \varepsilon = \frac{A^2}{6}\,\underset{\sim}{b}_i^T\,\underset{\sim}{b}_i\,\bar{\varepsilon} \tag{16}$$

where the factor ε remains to be determined.

An important question in the application of the hourglass control procedure is the selection of the parameter $\hat{\alpha}$ which relates the generalized gradient and flux, $\hat{g}$ and $\hat{q}$. In linear problems, the question has been examined in [12]. The following are the major results:

i. for $\bar{\varepsilon} = 1$, the element conductance matrix for a rectangular element coincides with the conductance matrix obtained by exact integration of (3).

ii. for $\bar{\varepsilon} = 3$, the assembly of the element conductance matrices at an interior point of a uniform rectangular mesh gives the standard 5-point finite difference stencil for the Laplacian.

iii. for $\bar{\varepsilon} = 2$, the assembly of the element conductance matrix for a uniform, square mesh gives the standard 9-point finite difference stencil for the Laplacian.

iv. the rate of convergence of all of the above is approximately like h^2, but $\bar{\varepsilon} = 2$ gives the best absolute accuracy in the problems studied. Moreover, if ε is a small number like 10^{-2}, the rate of convergence is still of the order h^2.

The result (iv) implies that the rate of convergence for the quadrilateral for one-point and 2 x 2 quadrature is the same; i.e. that the use of reduced integration in this case does not decrease the rate of convergence. Based on these results, it appears that from a practical viewpoint, one alternative is to let $\hat{\alpha} = \varepsilon\alpha$ with ε a small number. However, numerical studies suggest that for the Laplace operator a value of $\bar{\varepsilon}$ between 1 and 2 works best but that in continuum mechanics, small values should be used. In nonlinear problems, $\hat{\alpha}$ then simply becomes a variable which is directly proportional to α. It can be shown by a Hu-Washizu type variational principle that this choice of the parameters $\hat{\alpha}$ is consistent also in a mechanical sense.

3. SOLID MECHANICS

In solid mechanics, the rank deficiency of the 1 point quadrature quadrilateral is 2 in two dimensions and 12 in three dimensions. The corresponding number of additional generalized strains which meet the consistency requirements can be shown to be

$$\dot{q}_{i\alpha} = \underset{\sim}{\gamma}_\alpha^T\,\dot{\underset{\sim}{u}}_i^e \tag{17}$$

$$\underset{\sim}{\gamma}_\alpha = \frac{1}{\Omega}\,[\underset{\sim}{h}_\alpha - (\underset{\sim}{h}_\alpha^T\,\underset{\sim}{x}_j)\,\underset{\sim}{b}_j] \tag{18}$$

where $\Omega = A$ or V and the range of α is 1 or 4 for 2D or 3D, respectively. The matrices $\underset{\sim}{h}$ and $\underset{\sim}{b}$ are defined for 3D in [11].

The nodal forces are given by

$$f_{iI} = V(B_{jI}\,\sigma_{ij} + \gamma_{\alpha I}\,Q_{\alpha i}) \qquad Q^\nabla_{\alpha i} = G_{ij}\,\dot{q}_{\alpha j} \tag{19}$$

where $\underset{\sim}{\sigma}$ is the stress matrix and $\underset{\sim}{Q}^\nabla$ a frame invariant rate given by

$$Q_i^{\nabla} = \dot{Q}_i - W_{ij} Q_j \qquad W_{ij} = \frac{1}{2}(\dot{u}_{i,j} + \dot{u}_{j,i}) \qquad (20)$$

4. NUMERICAL RESULTS

The purpose of these examples is: 1) the show that hourglass control is necessary obtain reasonable solutions with one-point quadrature, 2) to examine the performance of the variable hourglass parameters in nonlinear problems.

Results are given for the circular domain shown in Fig. 1. Four-fold symmetry was used. The parameters are: radius = 5.0; $\alpha = 0.04$, $u(\underset{\sim}{x},0) = 0.1$. The outer boundary is insulated. A point source with the time history shown in Fig. 1 is applied at the center node.

The solution was obtained by explicit time integration. Figure 2 shows a plot of the results with $\varepsilon = 0$, which corresponds to one-point quadrature with no stabilization. As can be seen, the result exhibits severe oscillations due to the rank-deficiency of the element.

The solution was then obtained for a nonlinear problem where $\alpha(u) = \alpha_0 (1. + 0.01u^{1.4})$; $\alpha_0 = 0.04$. Four cases were considered: (1) $\hat{\alpha} = \varepsilon\alpha_0$; $\bar{\varepsilon} = 1.0$, (2) $\hat{a} = \varepsilon\alpha$; $\bar{\varepsilon} = 1.0$, (3) $\hat{a} = \varepsilon a$; $\bar{\varepsilon} = 0.1$, (4) $\hat{\alpha} = \varepsilon a$; $\bar{\varepsilon} = 2.0$. The parameter $\bar{\varepsilon}$ is given in terms of ε by Eq. (23.b). Selected results are shown in Fig. 3. As can be seen, case 1, which fails to account for the change in α, is substantially in error. Cases 2 and 4 agree quite well and with a more precise numerical solution which is not shown. Case 3 is not as much in error as Case 1 but is still quite poor. It can be concluded that using small values of $\bar{\varepsilon}$ to stabilize the mesh is not completely satisfactory, but values of order of magnitude 1.0 to 2.0 yield good results when $\hat{\alpha}$ varies with α.

ACKNOWLEOGEMENT

The support of the National Science Foundation under Grant CEE-8211862 is gratefully acknowledged. This paper is a condensed version of Ref. [16] which is being presented at the 1983 Summer Annual Meeting of the Applied Mechnaics Division of the American Society of Mechanical Engineers.

REFERENCES

1. GOUDREAU, G.L., HALLQUIST, J.O., "Recent Developments in Large Scale Finite Elements Lagrangian Hydrocode Technology", Report UCRL-86460, Lawrence Livermore Laboratory, October 1981, to be published in the Computer Methods in Applied Mechanics and Engineering, 1982.

2. BELYTSCHKO, T., ROBINSON, R.R., "SAMSON2: A Nonlinear Two-Dimensional Structure/Media Interaction Computer Code", Report AFWL-TR-81-109, Kirtland AFB, New Mexico, November 1981.

3. KULAK, R.F., "A Finite Element Formulation for Fluid-Structure Interaction in Three-Dimensional Space", Journal of Pressure Vessel Technology, Vol. 1D3, 1981, pp. 183-190.

4. WILKINS, M.L., BLUM, R.E., CRONSHAGEN, E., GRANTHAM, P., "A Method for Computer Simulation of Problems in Solids Mechanics and Gas Dynamics in Three Dimensions and Time" Lawrence Livermore Laboratory, Report UCRL-51574, Revision 1, May 1975.

5. BELYTSCHKO, T., KENNEDY, J.M., SCHOEBERLE, D.F., "On Finite Element and Difference Formulations of Fluid Structure Problems", Proc. of the Conf. on Computer Methods in

Nuclear Engineering, Charleston, S.C., 4:39-51, 1975.

6. MAENCHEN, G., SACK, S., "The TENSOR Code", in Methods in Computational Physics, Vol. 3, Ed. by B. Alder et al., Academic Press, 1964, pp. 181-210.

7. IRONS, B., AHMAO, S., Techniques of Finite Elements, Ellis horwood, Chichester, England, 1980.

8. BELYTSCHKO, T., KENNEDY, J.M., "Computer Models for Subassembly Simulation", Nuclear Engineering and Design, Vol. 49, July 1978, pp. 17-38.

9. KEY, S.W., "A finite element procedure for the large deformation dynamics response of axisymetric solids", Computer Methods in Applied Mechanics and Engineering, 4, 195-218, 1974.

10. KOSLOFF, D., FRAZIER, G.A., "Treatment of hourglass patterns in low order finite element codes", Interational Journal for Numerical and Analytical Methods in Geomechanics, 2, 57-72, 1978.

11. FLANAGAN, D.P., BELYTSCHKO, T., "A Uniform Strain Hexahedron and Quadrilateral with Orthogonal Hourglass Control", International Journal for Numerical Methods in Engineering, Vol. 17, pp. 679-706, 1981.

12. IRONS, B.M., RAZZAQUE, A., "Experience with the Patch Test for Convergence of Finite Elements in the Mathematical Foundations of the Finite Element Method with Applications to Partial Differential Equations", Ed. by A.K. Aziz, Academic Press, 1972, pp. 589-602.

13. STRANG, G., "Variational Crimes in the Finite Element Method", ibid, pp. 689-710.

14. ZIENKIEWICZ, O.C., The Finite Element Method, 3rd Edition, McGraw-Hill, 1977.

15. LIU, W.K., BELYTSCHKO, T., "Efficient Linear and Nonlinear Heat Conduction with a Quadrilateral Element", submitted for publication.

16. BELYTSCHKO, T., LIU, W.K., KENNEDY, J.M., "Hourglass Control in Linear and Nonlinear Problems", Recent Development in Computing Methods for Nonlinear Structural Mechanics, ed. by S. Atluri and N. Perrone, American Society of Mechanical Engineers, Houston, 1982.

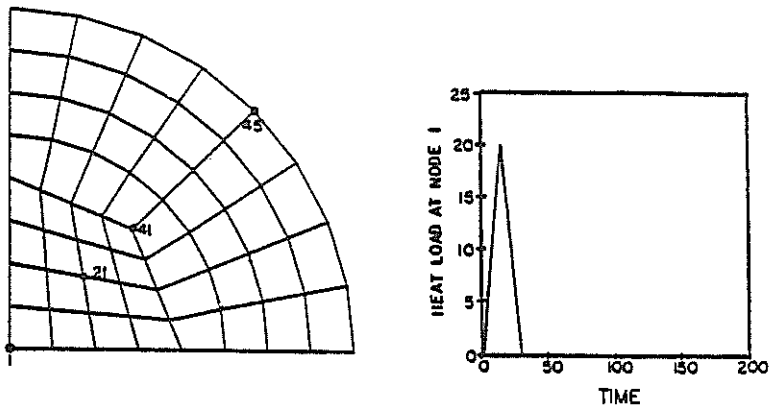

Fig.1. Mesh for example problem and time history of heat source at node 1.

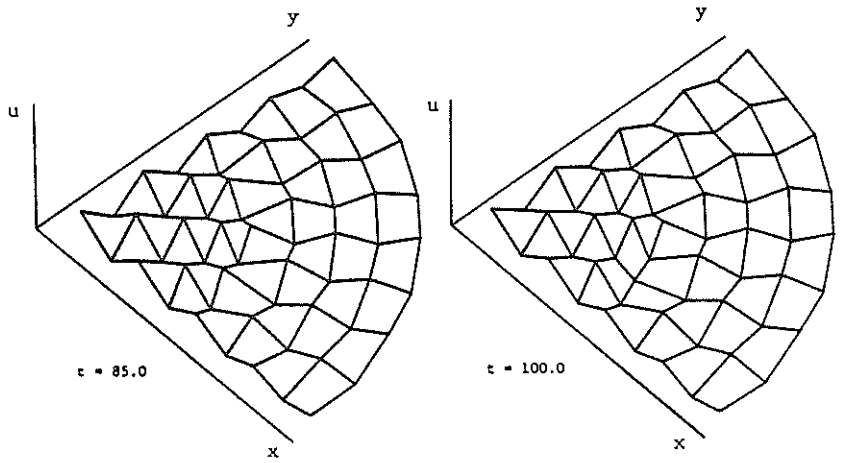

Fig.2. Plot of dependent variable u showing development of mesh instability when $\varepsilon = 0$.

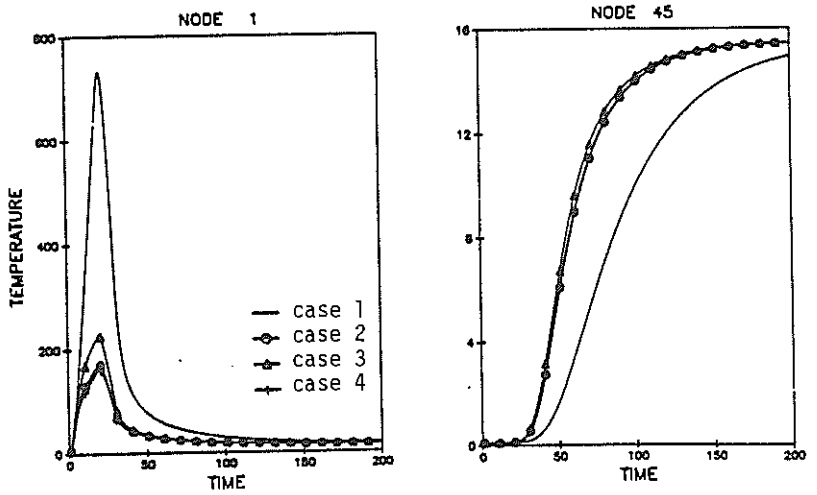

Fig. 3. Time histories for cases 1 to 4 at nodes 1 and 45.